

Three-Dimensional Tomographic Reconstruction of CR-2219 and CR-2223

D.G. Lloveras¹ A.M. Vásquez¹ F.A. Nuevo¹
N. Sachdeva² W. Manchester IV² B. Van der Holst²
R.A. Frazin² P. Lamy³ H. Gilardy³

¹Instituto de Astronomía y Física del Espacio (IAFE)
CONICET – University of Buenos Aires, Buenos Aires, Argentina

²Department of Climate and Space Sciences and Engineering (CLaSP),
University of Michigan, Ann Arbor, MI, USA

³Laboratoire Atmosphères, Milieux et Observations Spatiales, CNRS & UVSQ, Guyancourt, France

WHPI-Workshop — September 14th, 2021

- Interest in predicting space weather conditions constantly pushes the advance of state-of-the-art of 3D-MHD models, which need to be validated with observational data.
- Solar rotational tomography (SRT) provides a 3D empirical description of the inner solar atmosphere in a global fashion.
- We carry out SRT reconstructions of two WHPI targets:
 - CR-2219 (Total Solar Eclipse Campaign)
 - CR-2223 (PSP/STEREO-A Closest Approach)
- Using AIA images (in 171, 193 and 211 Å), we apply DEM-Tomography to reconstruct N_e and T_e , in the range of heights $\approx 1.0 - 1.25 R_\odot$.
- Using LASCO-C2 images, we apply VL-Tomography reconstruct N_e , in the range of heights $\approx 2.5 - 6.0 R_\odot$.
- We also ran steady-state simulations of both periods using the SWMF/AWSOM model (Univ. of Michigan).

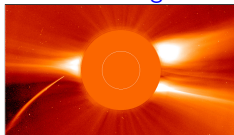
Solar Rotational Tomography (SRT)

The object of study is the Solar Corona.
Solar rotation provides the multiple viewpoints.

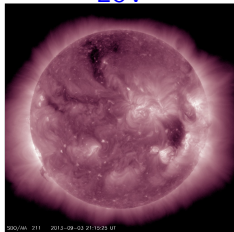
- **K-Corona:** Thomson scattered VL.
- **SRT-VL** → 3D N_e .
- 1st SRT-VL: Altschuler & Perry (1972)

- **E-Corona:** coronal emission: UV, EUV.
- **SRT-EUV** → 3D EUV emissivity →
3D Differential Emission Measure →
3D N_e y T_e
- 1st SRT-EUV (or **DEM-Tomography**):
Frazin, Vásquez & Kamalabadi (2009)
Vásquez, Frazin & Kamalabadi (2009)

Visible Light

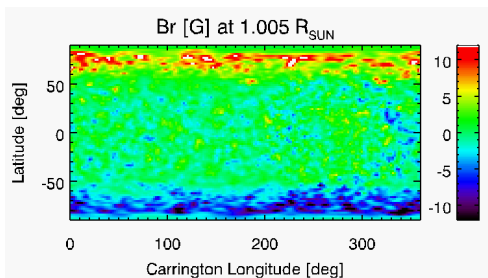


EUV



MHD-3D AWSoM model

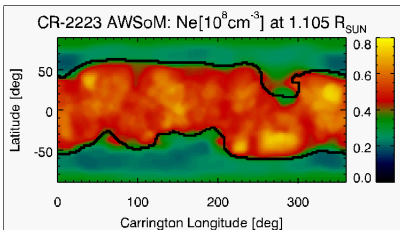
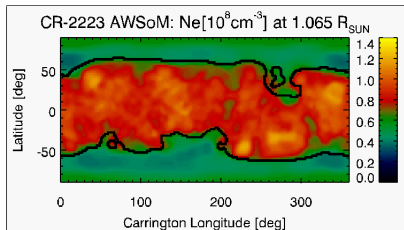
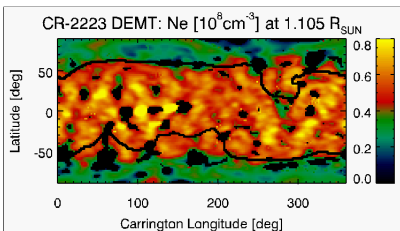
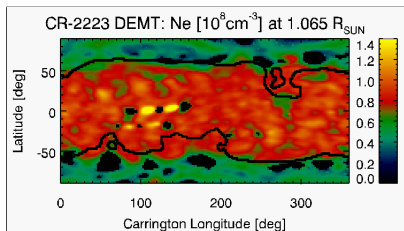
- MHD-3D: Alfvén-Wave driven Solar wind Model (AWSoM), within the Space Weather Modeling Framework (SWMF).
- Coronal heating given by dissipation of Alfvén waves (van der Holst et al., 2014).
- Spans from the chromosphere up to 1 AU.
- Synoptic Magnetogram as Boundary Condition (ADAPT-GONG).



Sachdeva et al. (2019), ApJ

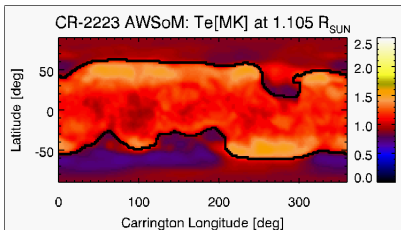
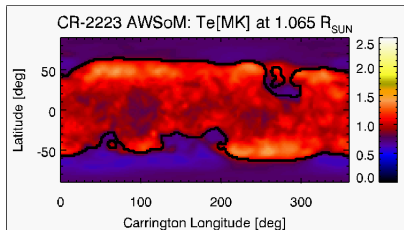
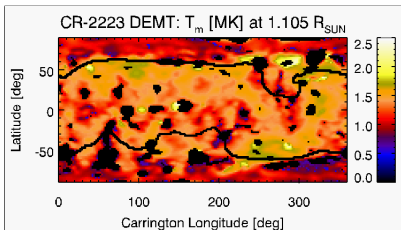
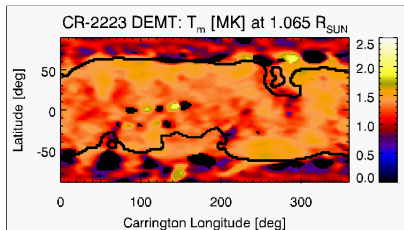
Lloveras et al. (2017, 2020), Sol.Phys.

N_e : DEMT versus AWSoM



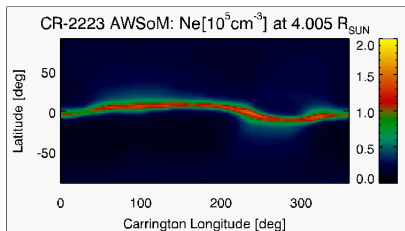
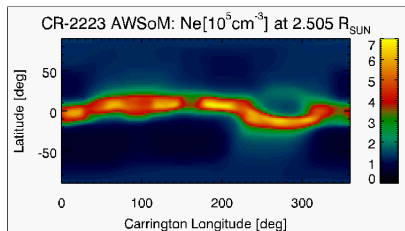
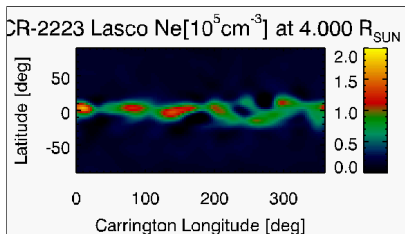
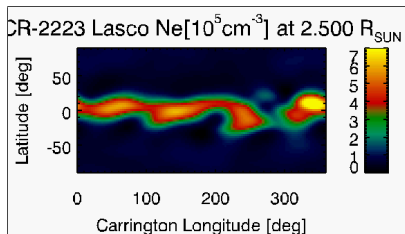
Latitude/longitude maps of N_e at two sample heights
from **DEMT** (top) and **AWSoM** (bottom).

T_e : DEMT versus AWSoM



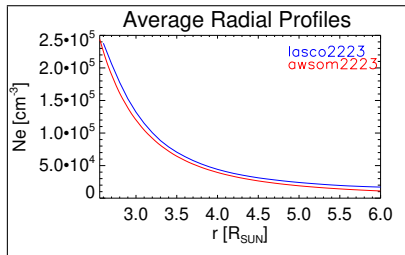
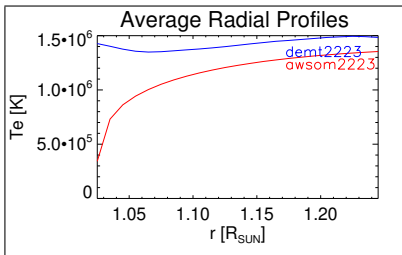
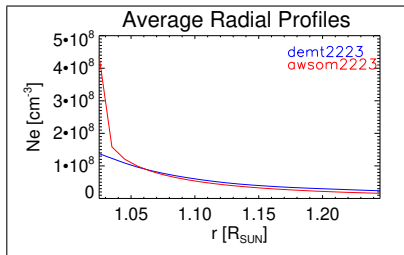
Latitude/longitude maps of T_e at two sample heights
from **DEMT** (top) and **AWSoM** (bottom).

N_e : SRT-WL versus AWSoM



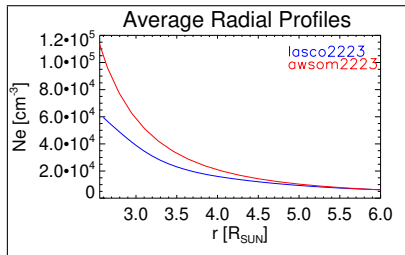
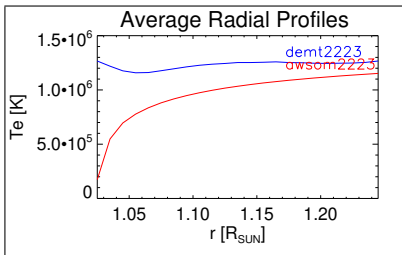
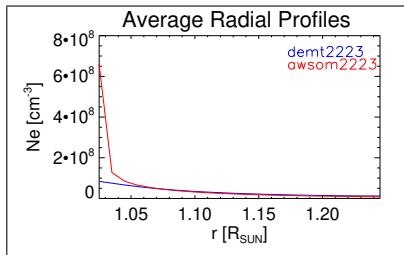
Latitude/longitude maps of N_e at two sample heights
from **SRT-WL** (top) and **AWSoM** (bottom).

Streamer Average Radial Profiles



$N_e(r)$ and $T_e(r)$ from **DEMT** and **AWSOM** (top).
 $N_e(r)$ from **SRT-WL** and **AWSOM** (bottom).

CHs Average Radial Profiles



$N_e(r)$ and $T_e(r)$ from **DEMT** and **AWSOM** (top).
 $N_e(r)$ from **SRT-WL** and **AWSOM** (bottom)

DEMT of CR-2081 (2008-2009)

Comparative Coronal Study of CR-1915 and CR-2081

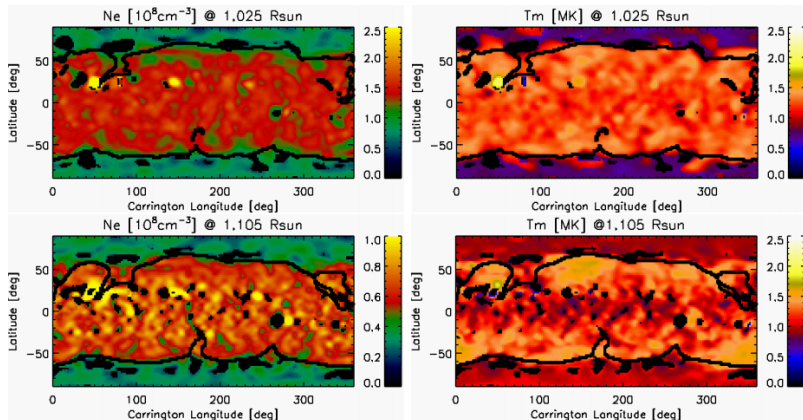
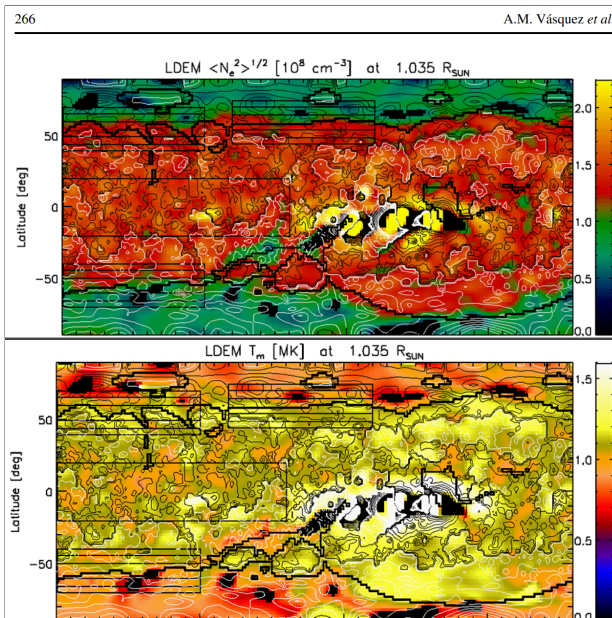
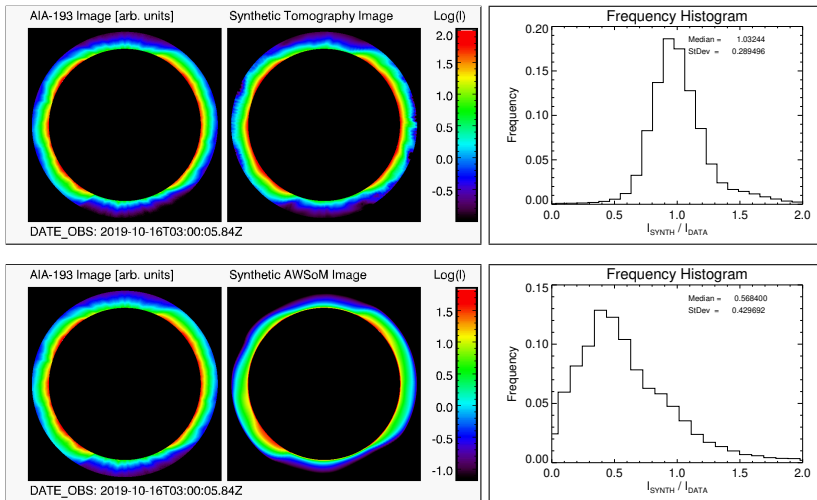


Figure 4. Same as Figure 3, but for CR-2081.



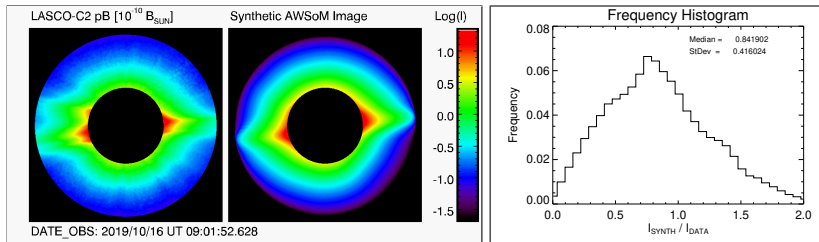
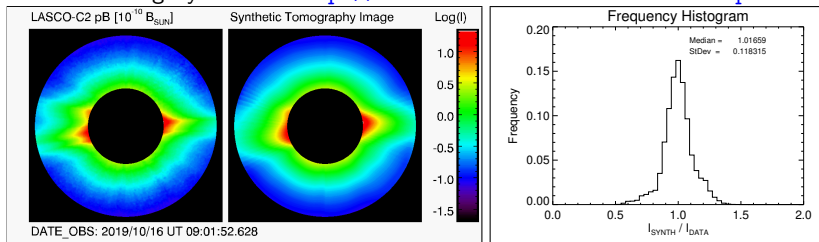
CR-2223 EUV Images: Data versus Synthetic



AIA 193 Å and corresponding synthetic image, plus intensity-ratio histogram, from **Tomography** (top) and from the **AWSoM** model (bottom).

CR-2223 VL Images: Data versus Synthetic

LASCO-C2 Legacy Archive <http://idoc-lasco-c2-archive.ias.u-psud.fr>











LASCO-C2 and corresponding synthetic image, plus intensity-ratio histogram, from **Tomography** (top) and from the **AWSoM** model (bottom).

Conclusions

- Characteristic values of N_e and T_e in the AWSoM model are consistent with the tomographic reconstructions.
- **Streamer:** within the FoV of AIA the model $N_e(r)$ agrees very well with the tomographic reconstructions, while the model $T_e(r)$ is $\approx 15\%$ smaller than in the reconstructions. **HCS:** within the FoV of LASCO-C2, the model $N_e(r)$ agrees very well with the reconstructions.
- **CHs:** within the FoV of AIA the model $N_e(r)$ agrees very well with the tomographic reconstructions, while the model $T_e(r)$ is $\approx 15\%$ smaller than in the reconstructions. Within the FoV of LASCO-C2, the model tends to overestimate $N_e(r)$ and underestimate its scale height.
- As a test for both the tomographic reconstructions and the AWSoM model, we synthesize images from both and compare them with the AIA and LASCO-C2 data. As expected, tomographic reconstructions are able to reproduce images with much finer detail than the model.
- An upcoming publication will include a detailed quantitative analysis for both CR-2223 and CR-2219, similar to [Lloveras et al. \(2020\)](#), *Sol.Phys.* 295, 76.

DATA PRODUCT we are sharing through HSO Connect

Shared with me > WHPI_Tomography ▾ 👤

| Name | Owner | Last modified | ↓ | File size |
|--|----------------|---------------|----|-----------|
|  README.txt 👤 | me | 9 Sept 2021 | me | 748 bytes |
|  read_tomography.pro 👤 | Federico Nuevo | 9 Sept 2021 | me | 4 KB |
|  Te_EUV-Tomography_CR2219_rmin1.02_rmax1.25 👤 | me | 9 Sept 2021 | me | 1.4 MB |
|  Te_EUV-Tomography_CR2223_rmin1.02_rmax1.25 👤 | me | 9 Sept 2021 | me | 1.4 MB |
|  Ne_EUV-Tomography_CR2223_rmin1.02_rmax1.25 👤 | me | 9 Sept 2021 | me | 1.4 MB |
|  Ne_EUV-Tomography_CR2219_rmin1.02_rmax1.25 👤 | me | 9 Sept 2021 | me | 1.4 MB |
|  Ne_VL-Tomography_CR2219_rmin2.45_rmax6.05 👤 | me | 9 Sept 2021 | me | 1,013 KB |
|  Ne_VL-Tomography_CR2223_rmin2.45_rmax6.05 👤 | me | 9 Sept 2021 | me | 1,013 KB |